Jets, W/Z and Top Quark Production at the LHC and Status of the Higgs Boson Searches at ATLAS

Oliver Kortner on behalf of the ATLAS and CMS collaborations

Max-Planck-Institut für Physik, Föhringer Ring 6, 80806 Munich, Germany

DOI: `http://dx.doi.org/10.3204/DESY-PROC-2012-02/25`

Until the end of 2011 the ATLAS and CMS experiments have each analysed up to 5 fb^{-1} of pp collision data at $\sqrt{s} = 7$ TeV. Their studies show excellent agreement between Standard Model predictions and experimental measurements for the production of jets, W/Z bosons, and top quarks. The ATLAS experiment has been able to exclude a Standard Model Higgs boson at 95% confidence level in the mass intervals 110 GeV $< m_H <$ 117.5 GeV, 118.5 GeV $< m_H <$ 122.5 GeV, 129 GeV $< m_H <$ 539 GeV.

1 Introduction

The Large Hadron Collider (LHC) has delivered about 5 fb^{-1} of pp collision data at $\sqrt{s} = 7$ TeV for each of the multipurpose detectors ATLAS and CMS [1, 2] in 2010 and 2011. The data recorded by ATLAS and CMS allow for the verification of Standard Model predictions for the production of jets, W and Z bosons as well as a detailed study of top quark production. The amount of data recorded provides sensitivity for a possible exclusion of a Standard Model Higgs boson over a wide expected mass range, from 120 GeV up to about 555 GeV at 95% confidence level. This note summarizes the status of the studies of jets, W/Z, and top quark production by ATLAS and CMS and the status of the Standard Model Higgs searches of the ATLAS experiment.

2 Jet production at the LHC

In proton proton collisions at the LHC, predominantly jets are produced via the strong interaction. The study of inclusive jet and di-jet production therefore probes next-to-leading order (NLO) perturbative QCD and the parton distribution functions. ATLAS and CMS have measured inclusive jet and di-jet cross sections. They both use the anti-k_T algorithm [3] to reconstruct jets, ATLAS with the size parameter $R = 0.4$ and $R = 0.6$, CMS with $R = 0.7$. ATLAS considers jets up to absolute values of rapidities of 4.4 while CMS stops at 2.5 in the inclusive jet and dijet studies [4, 5, 6]. ATLAS probes transverse jet momenta between 20 GeV and 1.5 TeV in the inclusive measurement and di-jet masses between 70 GeV and 5 TeV. CMS considers jets with transverse momenta between 18 GeV and 2 TeV and di-jet masses between 200 GeV and 5 TeV. The studies are therefore sensitive to values of x, the momentum fraction carried by the colliding partons, between 10^{-4} and 0.5. Both experiments express their results

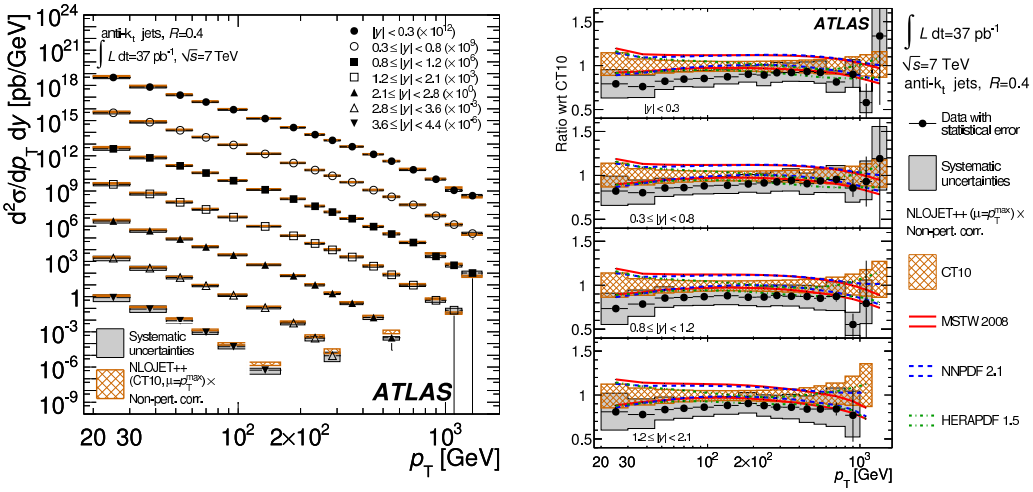

Figure 1: Left: Double differential inclusive jet production cross section measured by ATLAS. Right: Comparison of the ATLAS cross section measurements with NLO predictions corrected for non-perturbative effects [4].

in terms of jets at particle level and apply non-perturbative corrections to the NLO predictions which are important at jet transverse momenta below 100 GeV.

Figure 1 shows a comparison of the double differential inclusive jet production cross section measured by ATLAS with NLO predictions for anti-k_T jets with $R = 0.4$. The experimental data agree with NLO QCD predictions within the experimental and theoretical uncertainties in the entire phase space probed. Better agreement between experimental data and predictions is obtained for large jet sizes [4, 6].

In Figure 2 the double differential di-jet production cross section measured by CMS is compared with NLO predictions. Like in the case of the inclusive jet production cross section, the experimental data are in agreement with the theoretical predictions within the experimental and theoretical uncertainties.

3 Production of W and Z bosons at the LHC

3.1 Inclusive W and Z production mechanisms

W and Z bosons are created in quark antiquark collisions at the LHC. W^+ bosons are produced in collisions of u type quarks and d type antiquarks; in lowest order of perturbation theory, about 80% of the W^+ bosons are produced in $u\bar{d}$ collisions, about 20% in $c\bar{s}$ collisions. W^- bosons are produced in collisions of d type quarks and u type antiquarks, in about 70% of all cases in $d\bar{u}$ collisions, in the remaining case mainly in $s\bar{c}$ collisions. As a proton contains two valence u quarks and one valence d quark, roughly two times more W^+ than W^- bosons are produced in pp collisions at the LHC. Z bosons are predominantly produced in $u\bar{u}$ and $d\bar{d}$ annihilations each in about 40% of the cases and in $s\bar{s}$ and, with smaller rate, $c\bar{c}$ annihilations in the remaining cases. Given the different coupling of the quark currents to W and Z bosons

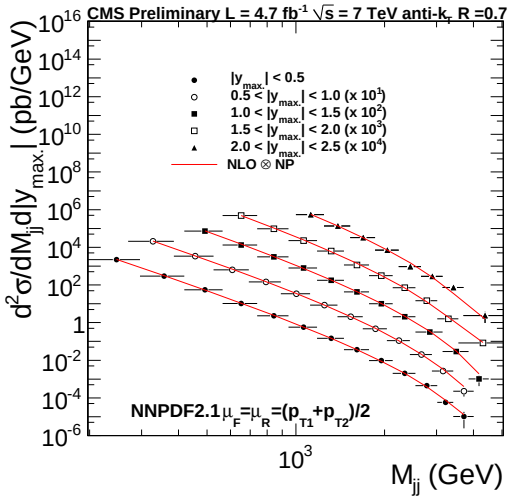

Figure 2: Comparison of double differential di-jet production cross section measured by CMS with NLO predictions corrected for non-perturbative effects [6].

more W than Z bosons are created [7]. The study of the W and Z production cross sections probes the parton densities at values of x in the interval $10^{-3} \lesssim x \lesssim 0.1$ where the momentum fractions $x_{1,2}$ of the colliding quark and antiquark are related to the W/Z rapidity by the $x_{1,2} = \frac{m_{W/Z}}{\sqrt{s}} e^{\pm y_{W/Z}}$ at tree level.

3.2 Selection of W and Z events

The ATLAS and CMS experiments use a similar selection to collect W and Z events which is driven by the final state topologies [8, 9]. W bosons are studied in their decays into a highly energetic isolated charged lepton (electron or muon) and the corresponding neutrino leading to significant missing transverse energy E_T^{miss}. The charged leptons are used to trigger the data acquisition. The E_T^{miss} distributions are used to determined the QCD background which are difficult to model with sufficient Monte-Carlo statistics. ATLAS requires $E_T^{miss} > 25$ GeV in the determination of the fiducial cross section because of the small background contribution to this phase space region. CMS does not impose an E_T^{miss} cut, but extracts the W yield from a template fit to the E_T^{miss} distribution.

Z bosons are identified by the two oppositely charged isolated high p_T decay leptons (electrons or muons). One or both charged leptons are used in the trigger. The main studies of the Z production are limited to the acceptance of the inner tracking system ($|\eta| \lesssim 2.5$); however the ATLAS experiments also considered topologies where one of the electrons is detected in the forward region ($|\eta| < 4.9$) with calorimetric coverage [8]. The results of this measurement with extended acceptance are in agreement with the main studies.

3.3 Measurements of the W and Z cross sections

Table 1 summarizes the measurements of the $W^{\pm}$ and Z productions cross sections by ATLAS and CMS based on an integrated luminosity of about 35 pb^{-1} per experiment; (Drell Yan) lepton pair production via a virtual photon are taken into account in the Z analysis. The cross sections which have been measured with similar accuracy by the two experiments agree within the quoted uncertainties. They are also in good agreement with the NNLO predictions of (6.15 ± 0.17) nb for W^+, (4.29 ± 0.11) nb for W^-, and (0.97 ± 0.03) nb for Z/γ^* [9] which are obtained with FEWZ [10] and the MSTW 2008 parton density function [11].

	$\sigma_W^{tot} \cdot \mathrm{BR}(W \to \ell\nu)$ [nb]							
	ATLAS				CMS			
	stat	sys	lum	acc	stat	sys	lum	acc
W^+	$6.048 \pm 0.016 \pm 0.072 \pm 0.206 \pm 0.096$				$6.04 \pm 0.02 \pm 0.06 \pm 0.24 \pm 0.08$			
W^-	$4.160 \pm 0.014 \pm 0.057 \pm 0.141 \pm 0.083$				$4.26 \pm 0.01 \pm 0.04 \pm 0.17 \pm 0.04$			
$W^{\pm}$	$10.207 \pm 0.021 \pm 0.121 \pm 0.347 \pm 0.164$				$10.31 \pm 0.02 \pm 0.09 \pm 0.41 \pm 0.10$			
	$\sigma_{Z/\gamma^*}^{tot} \cdot \mathrm{BR}(Z/\gamma^* \to \ell\ell)$ [nb]							
	ATLAS				CMS			
	stat	sys	lum	acc	stat	sys	lum	acc
Z/γ^*	$0.937 \pm 0.006 \pm 0.009 \pm 0.032 \pm 0.016$				$0.974 \pm 0.007 \pm 0.007 \pm 0.039 \pm 0.018$			

Table 1: Measured W and Z cross sections times branching ratios[8][9].

Higher sensitivity to the theoretical predictions is provided by differential cross sections. ATLAS and CMS find good agreement between their measured differential cross sections and the theoretical predictions. The plot on the left of Figure 3 shows the W^+ production cross section as a function of the pseudorapidity of the charged decay lepton as measured by the ATLAS experiment compared to predictions of the FEWZ [10] and DYNNLO[12] NLO calculations with different parton densities; the corresponding dependence of the Z production cross section on the rapidity of the Z boson is presented on the right of Figure 3. The measured distributions follow the predictions, but trends in the deviations of some parton density function sets are visible. The ATLAS results slightly favour MSTW08 [11] and slightly disfavour JR09 [13]. Improvements of the parton density functions by including these measurements can be expected.

3.4 Production of W and Z bosons in association with jets

W and Z bosons can be produced in association with jets (abbreviated to j in the following). Two basic processes are possible at lowest order: initial state gluon radiation of the colliding quarks and the radiation of a W or Z boson from one of the colliding quarks. The study of $W+j$ and $Z+j$ production is interesting as a test of QCD; the measurement of $W+c$ is sensitive to the s quark parton density function, the measurement of $Z+b$ to the b quark parton density function. Finally $W+j$ and $Z+j$ production is an important background to many physics processes, for instance to $pp \to t\bar{t}+X \to (W^+b)(W^-\bar{b})+X$ and $pp \to t+X \to (W^+b)+X$ or $pp \to H+X \to W^+W^-+X \to 2j+\ell\nu+X$.

Figure 4 summarizes the measurements of the $W+j$ [14] and $Z+j$ [15] cross sections and their comparisons with theoretical predictions. Good agreement with predictions of the jet multiplicity and jet kinematics by state-of-the art multi-parton matrix element generators like

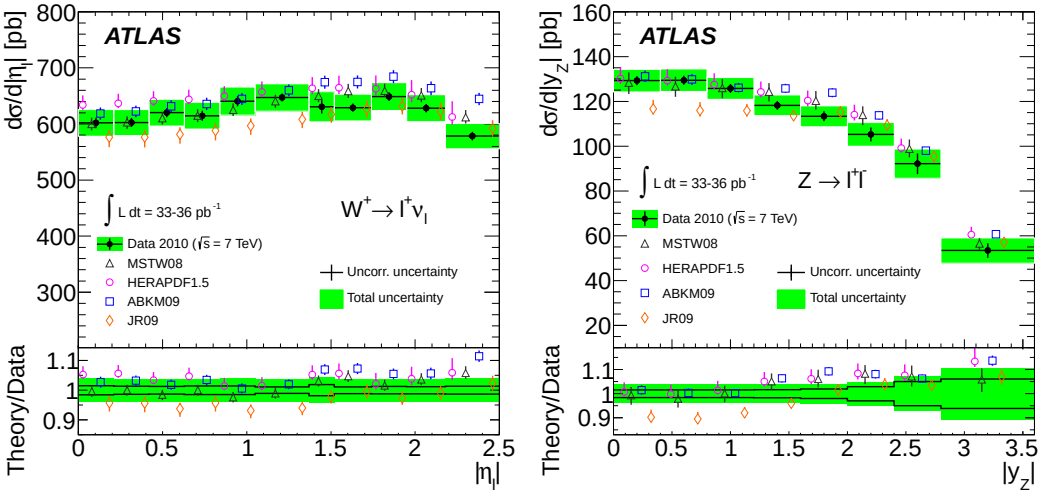

Figure 3: Comparison of differential cross sections measured by ATLAS with theoretical predictions by the FEWZ and DYNNLO calculations with different parton densities [8]. Left: W^+ production. Right: Z production.

ALPGEN [16] and SHERPA [17] is observed. PYTHIA [18] as leading order matrix element generator provides a good prediction for the production of one additional jet, but fails for higher jet multiplicities as expected.

3.5 Di-boson production

ATLAS and CMS have also studied the production of pairs of W and Z bosons. Figure 5 shows the lowest order Feynman diagrams for di-boson production. The continuum production of W and Z boson pairs is an important background to $H \to W^+W^-$ and $H \to ZZ$. In the Standard Model of electroweak interactions, the triple gauge boson vertex $Z/\gamma^* \to W^+W^-$ is allowed while the vertex $Z/\gamma^* \to ZZ$ is forbidden. Deviations of the measured ZZ production cross section could therefore be an indication for anomalous triple gauge boson couplings.

Neither ATLAS nor CMS have found deviations from the Standard Model predictions. Based on an integrated luminosity of 4.7 fb^{-1}, ATLAS measures $\sigma(W^+W^-) = [53.4 \pm 2.1(\text{stat}) \pm 4.5(\text{syst}) \pm 2.1(\text{lumi})]$ pb [19], CMS, based on an integrated luminosity of 1.1 fb^{-1}, $[55.3 \pm 3.3(\text{stat}) \pm 6.9(\text{syst}) \pm 3.3(\text{lumi})]$ pb [21] which agrees with the NLO Standard Model prediction of (45.1 ± 2.8) pb. An updated CMS measurement with the full 2011 data set can be found in [20]. The NLO Standard Model prediction of $\sigma(ZZ) = (6.5^{+0.3}_{-2.3})$ pb [22] is also consistent with the experimental measurements of $[7.2^{+1.1}_{-0.9}(\text{stat})^{+0.4}_{-0.3}(\text{syst}) \pm 0.3(\text{lumi})]$ pb by ATLAS [22] and $[3.8^{+1.5}_{-1.2}(\text{stat}) \pm 0.2(\text{syst}) \pm 0.2(\text{lumi})]$ pb by CMS [21]. It should be noted that the statistical and systematic errors of the measurements are still larger than the uncertainties of the theoretical predictions.

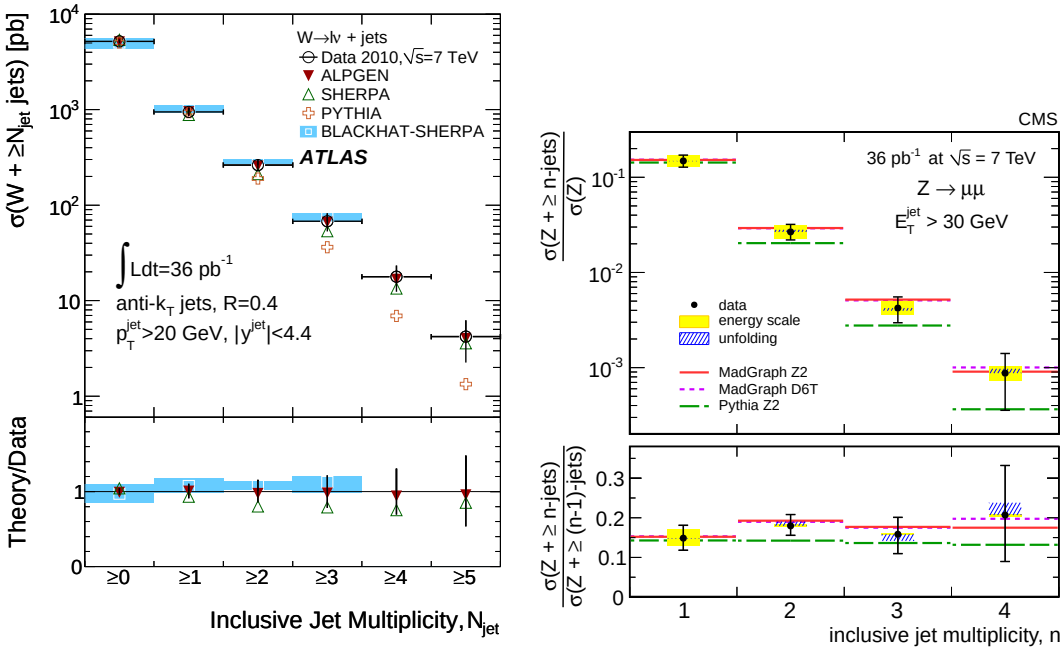

Figure 4: Comparison of the measured cross sections for the production of weak gauge bosons with jets as a function of the jet multiplicity. Left: $W + j$ as measured by ATLAS [14]. Right: $Z + j$ as measured by CMS [15].

4 Production of top quarks at the the LHC

At the LHC $t\bar{t}$ pairs are produced with a predicted cross section of 167^{+17}_{-18} pb mainly via gluon fusion [23]. Production of single top quarks is also possible at the LHC via t channel production ($64.6^{+3.3}_{-2.6}$ pb) [24], associated Wt production ($15.7^{+1.3}_{-1.4}$ pb) [25], and s channel production ((4.6 ± 0.3) pb) [26] as depicted in the Feynman diagrams of Figure 6. The experimental signature of the top quark decays is a b quark jet and the decay products of the W bosons produced in the top decay.

The LHC experiments have reached a precision of the $t\bar{t}$ cross section measurement which is smaller than the uncertainties of the theoretical predictions. Figure 7 shows a summary of the ATLAS and CMS measurements which are compatible with the theoretical predictions.

The statistics of $t\bar{t}$ pairs created at the LHC allows measurements of differential cross sections. Figure 8 shows as an example the dependence of the $t\bar{t}$ cross section of the rapidity of the $t\bar{t}$ systems. The measured cross section agrees with the theoretical predictions in all rapidity bins. The experiments have also found good agreement of the experimental measurements of the spin correlations in $t\bar{t}$ pairs [31] and the polarization of the W bosons in top quark decays [32, 33] with theoretical predictions.

ATLAS and CMS have also studied the production of single top quarks. Given the small cross sections the analysed amount of data of about 1 fb^{-1} allowed only for the measurements of the t channel and Wt production cross sections. ATLAS measures $\sigma(\text{t channel}) = 90^{+32}_{-22}$ pb [34]

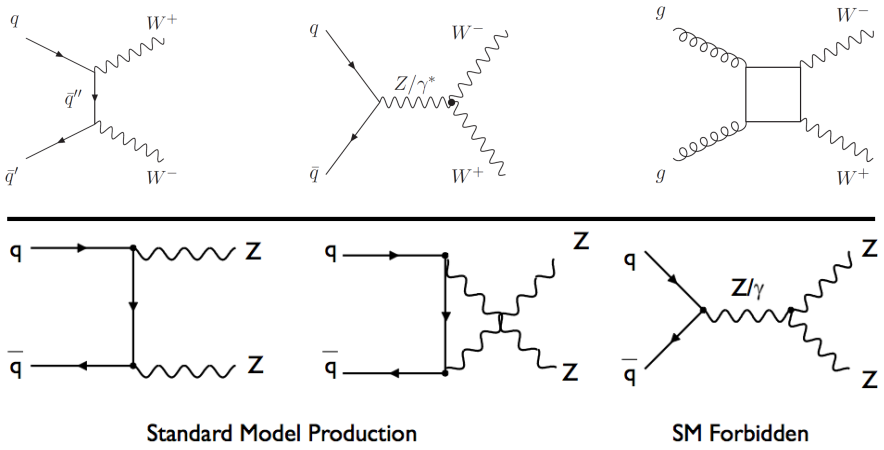

Figure 5: Lowest order Feynman diagrams for di-boson production. The graph on the bottom right is forbidden in the Standard Model.

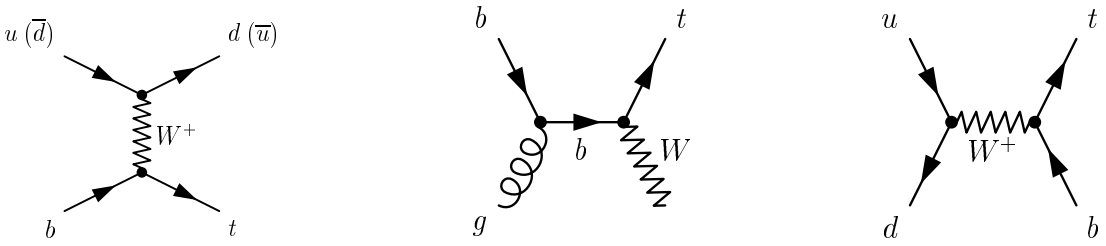

Figure 6: Lowest order Feynman diagrams of single top quark production. Left: t channel production. Middle: Wt production. Right: s channel production.

and $\sigma(Wt) < 39.1$ pb at 95% confidence level[35]; CMS finds σ(t channel) = [70.3$\pm$6.15(stat)$\pm$ 9.61(syst) $\pm$ 3.36(lumi)] pb [36] and $\sigma(Wt) = 22^{+9}_{-7}$ pb at 2.7σ significance [37]. The results are compatible with the theoretical predictions.

5 Status of the search for the Standard Model Higgs boson with the ATLAS detector at the LHC

Figure 9 shows the lowest order Feynman diagrams of the Standard Model Higgs production mechanisms which are exploited by the Higgs searches of the ATLAS experiment. At the LHC Standard Model Higgs bosons are predominantly produced in gluon gluon fusion. Over a wide mass range the vector boson fusion process is an order of magnitude less frequent, but its final state topology with two high p_T forward jets with a large rapidity gap and the Higgs decay products in this gap allows for a powerful background suppression which is needed for the $H \to \tau\tau$ channel in particular. The production of Higgs bosons in association with W/Z bosons has an even lower cross section; it used in the $H \to b\bar{b}$ channel to suppress the large inclusive $b\bar{b}$ background.

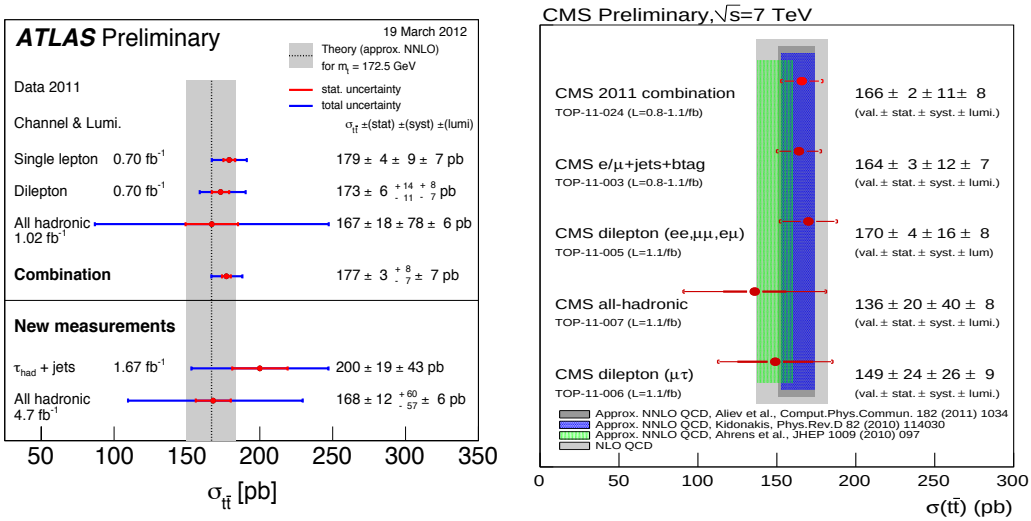

Figure 7: Summaries of the measurements of the $t\bar{t}$ production cross sections by ATLAS (left) [27, 28] and CMS [29] (right).

The integrated luminosity of 4.7 fb^{-1} collected by the ATLAS experiment makes it possible to exclude the Standard Model Higgs boson with $> 95\%$ confidence level over a wide range of Higgs masses m_H; the expected exclusion intervall is $m_H \in [120\text{ GeV}, 555\text{ GeV}]$ as presented in Figure 10. For $m_H \gtrsim 150$ GeV the exclusion is dominated by the following channels:

- $m_H \gtrsim 300$ GeV: $H \to ZZ \to \ell\ell\nu\nu$;
- 200 GeV $\lesssim m_H \lesssim 300$ GeV: $H \to ZZ \to 4\ell$;
- 150 GeV $\lesssim m_H \lesssim 200$ GeV: $H \to WW^* \to \ell\ell\nu\nu$.

The channel $H \to WW^* \to \ell\ell\nu\nu$ is still the most sensitive channel down to $m_H \approx 130$ GeV. At lower Higgs masses, one needs to combine it with the following channels to reach sensitivity to the Standard Model cross section:

- $H \to ZZ^* \to 4\ell$;
- $H \to \gamma\gamma$;
- $H \to \tau\tau$ in vector boson fusion production;
- $H \to b\bar{b}$ in associate production with W and Z bosons.

ATLAS is able to exlude the following masses of the Standard Model Higgs boson [38]:

- 110 GeV $< m_H <$ 117.5 GeV, 118.5 GeV $< m_H <$ 122.5 GeV, 129 GeV $< m_H <$ 539 GeV at 95% confidence level;
- 130 GeV $< m_H <$ 486 GeV at 99% confidence level.

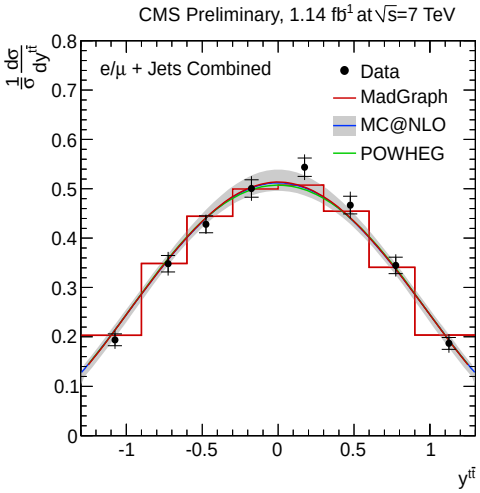

Figure 8: $t\bar{t}$ production as a function of the rapidity of the $t\bar{t}$ system as measured by CMS in comparison with NLO predictions [30].

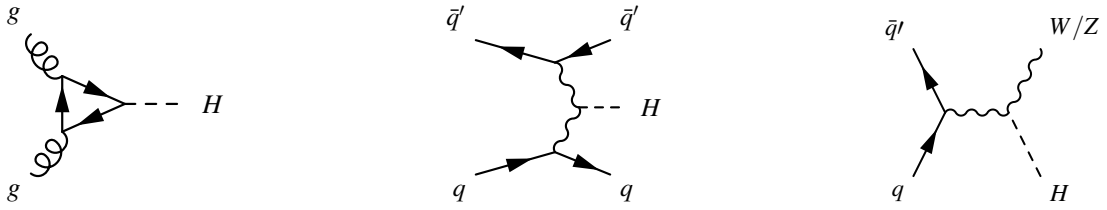

Figure 9: Lowest order Feynman diagrams of the Standard Model Higgs boson production mechanisms exploited by the ATLAS Higgs analyses. Left: Gluon gluon fusion. Middle: Vector boson production. Right: Associated Higgs production.

The observed exclusion limit around $m_H = 126$ GeV is worse than expected. This is caused by an excess of events over the background expectation in the $H \to \gamma\gamma$ and $H \to ZZ \to 4\ell$ channels. As shown in Figure 11, the excess has a 2.9 standard deviations local significance in the $H \to \gamma\gamma$ channel and a 2 standard deviations local significance in the $H \to ZZ^* \to 4\ell$ channel. As no excess is observed in the other channels, especially in the $H \to WW \to \ell\ell\nu\nu$ channel, the excess has a reduced local significance of 2.5 standard deviations. An excess of 2.9 standard deviations is expected for a Standard Model Higgs boson with $m_H = 126$ GeV. The best fit signal strength at $m_H \approx 126$ GeV is $0.9^{+0.4}_{-0.3}$ times the Standard Model cross section. The global probability of such a background fluctuation anywhere in the full explored mass range (110 GeV-600 GeV) is 30% and 10% in the mass range from 110 GeV to 146 GeV.

The triplication of the collected pp collision data in 2012 will make it possible to verify or falsify the existance of the Standard Model Higgs boson around $m_H = 126$ GeV.

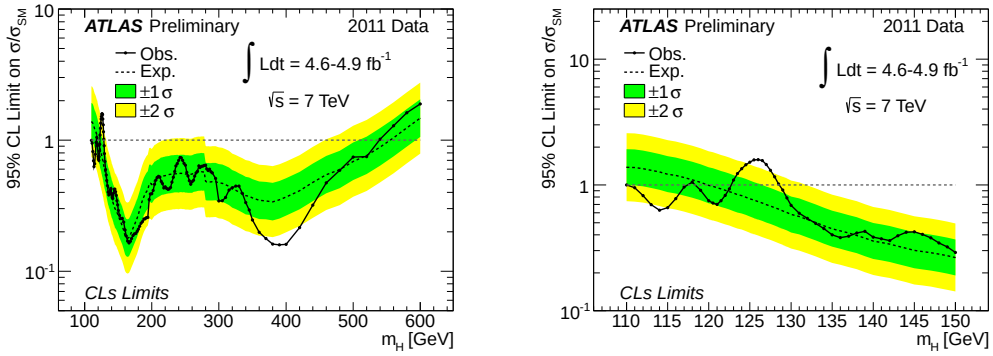

Figure 10: Exclusion limits for the Standard Model Higgs boson at 95% confidence level for Higgs boson masses m_H in the range between 100 GeV and 600 GeV [38]. The plot on the right zooms into the low mass region below $m_H = 150$ GeV.

6 Summary

The precision measurements of the production of jets, W/Z bosons and top quarks performed by ATLAS and CMS on up to 5 fb^{-1} of pp collisions data at $\sqrt{s} = 7$ TeV per experiment are in agreement with the prediction of the Standard Model. The experiment has been able to exclude a Standard Model Higgs boson at 95% confidence level in the mass intervals 110 GeV $< m_H <$ 117.5 GeV, 118.5 GeV $< m_H <$ 122.5 GeV, 129 GeV $< m_H <$ 539 GeV.

7 Bibliography

References

[1] ATLAS Collaboration, JINST 3 (2008) S08003.

[2] CMS Collaboration, JINST 3 (2008) S08004.

[3] M. Cacciari, G. Salam, and G. Soyez, JHEP 0804, 063 (2008), arXiv:0802.1189 [hep-ph].

[4] ATLAS Collaboration, arXiv:1112.6297.

[5] ATLAS Collaboration, ATLAS-CONF-2012-021, https://cdsweb.cern.ch/record/1430730.

[6] CMS Collaboration, CMS-PAS-QCD-11-004.

[7] A. D. Martin, R. G. Roberts, W. J. Stirling, R. S. Thorne, Eur.Phys.J.C14:133-145,2000.

[8] ATLAS Collaboration, Phys. Rev. D 85, 072004 (2012).

[9] CMS Collaboration, J. High Energy Phys. 10 (2011) 132.

[10] C. Anastasiou, L. J. Dixon, K. Melnikov, and F. Petriello, Phys. Rev. D 69, 094008 (2004).

[11] A. D. Martin, W. J. Stirling, R. S. Thorne, and G. Watt, Eur. Phys. J. C 63, 189 (2009).

[12] S. Catani and M. Grazzini, Phys. Rev. Lett. 98, 222002 (2007). S. Catani, L. Cieri, G. Ferrera, D. de Florian, and M. Grazzini, Phys. Rev. Lett. 103, 082001 (2009).

[13] P. Jimenez-Delgado and E. Reya, Phys. Rev. D 79, 074023 (2009).

[14] ATLAS Collaboration, Phys. Rev. D85 (2012) 092002.

[15] CMS Collaboration, J. High Energy Phys. 01 (2012) 010.

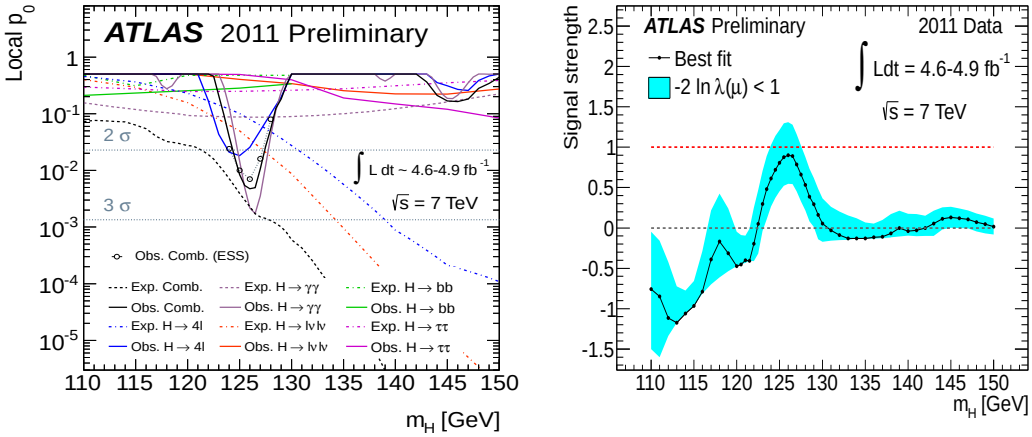

Figure 11: Left: Local statistical significance of an excess of events over the background expectation separate by Higgs decay channels. Right: Signal strength $\mu = \frac{\sigma}{\sigma_{SM}}$ best compatible with the observed excess. [38]

[16] M. L. Mangano et al., J. High Energy Phys. 07 (2003) 001.

[17] T. Gleisberg et al., J. High Energy Phys. 02 (2009) 007.

[18] T. Sjöstrand, S. Mrenna, and P. Skands, J. High Energy Phys. 05 (2006) 026.

[19] ATLAS Collaboration, ATLAS-CONF-2012-025, https://cdsweb.cern.ch/record/1430734.

[20] CMS Collaboration, CMS-PAS-SMP-12-005.

[21] CMS Collaboration, CMS-PAS-EWK-11-010.

[22] ATLAS Collaboration, ATLAS-CONF-2012-026, https://cdsweb.cern.ch/record/1430735.

[23] M. Aliev et al., Comput. Phys. Commun.182 (2011) 1034-1046, arXiv:1007:1327 [hep-ph].

[24] N. Kidonakis, Phys. Rev. D 83 (2011) 091503 [arXiv:1103.2792].

[25] N. Kidonakis, Phys. Rev. D 82 (2010) 054018 [arXiv:1005.4451].

[26] N. Kidonakis, Phys. Rev. D 81 (2010) 054028 [arXiv:1001.5034].

[27] ATLAS Collaboration, https://twiki.cern.ch/twiki/bin/view/AtlasPublic/CombinedSummaryPlots.

[28] ATLAS Collaboration, ATLAS-CONF-2012-024, https://cdsweb.cern.ch/record/1430733.

[29] CMS Collaboration, CMS-PAS-TOP-11-024.

[30] CMS Collaboration, CMS-PAS-TOP-11-013.

[31] ATLAS Collaboration, PRL 108, 212001 (2012).

[32] ATLAS Collaboration, ATLAS-CONF-2011-122, https://cdsweb.cern.ch/record/1376422.

[33] CMS Collaboration, CMS-PAS-TOP-11-020.

[34] ATLAS Collaboration, ATLAS-CONF-2011-101, https://cdsweb.cern.ch/record/1369217.

[35] ATLAS Collaboration, ATLAS-CONF-2011-104, https://cdsweb.cern.ch/record/1369829.

[36] CMS Collaboration, CMS-PAS-TOP-11-021.

[37] CMS Collaboration, CMS-PAS-TOP-11-022.

[38] ATLAS Collaboration, ATLAS-CONF-2012-019, https://cdsweb.cern.ch/record/1430033.